

Phantom-DRAWN: Direction Guidance using Rapid and Asymmetric Acceleration Weighted by Nonlinearity of Perception

Tomohiro Amemiya Hideyuki Ando Taro Maeda
NTT Communication Science Laboratories,
3-1 Morinosato Wakamiya, Atsugi-shi, Kanagawa, 243-0198, Japan
{t-amemiya, hide, maeda}@avg.brl.ntt.co.jp

Abstract

This paper describes the design of a novel force perception method and the development of a handheld force display based on the method. The method is based on the nonlinear characteristics of human tactile perception; humans feel rapid acceleration more strongly than slow acceleration. The method uses periodic prismatic motion to create asymmetric acceleration leading to a virtual force vector. A prototype of the handheld force display that generates one-directional force using a relatively simple mechanism was built, and its performance tested in terms of both physical and perceptual characteristics. We verify the feasibility of the proposed method through experiments that determine the display's motor's rotational frequency that maximizes the perception of the virtual force vector.

Key words: Force Display, Nonlinearity of Perception, Wearable and Mobile Computing, Non-grounded Device

1. Introduction

Too much information continues to invade our daily lives. Despite the limited information processing capacity of the human brain, previous studies on wearable information displays have continued to use visual and auditory channels, which are already overburdened. We focus on the force sensory channel (haptic channel) as a new channel for wearable information displays; this channel can be intuitively interpreted and provides long term location memory[1]. Since wearable force displays indicate direction, one of the most effective and researched application in wearable computers is navigation. Some navigation systems are based on cutaneous sensation as verbal information such as the cutaneous saltation on arm[2], shoulder tapping[3], and verbal information using Finger-Braille method[4]. Force displays, which are based on nonverbal information, are more suitable for intuitively presenting direction information for navigation than cutaneous ones. However, previous wearable and mobile force displays typically produce neither constant force nor translational force, without reaction force.

The method described in this paper, the first step in solving the problems of prior wearable and mobile force displays, is based on the asymmetric acceleration of a small mass with single DOF (degree of freedom). While our method does not provide an actual force, the virtual force sensation generated by the method is effectively perceived by the user as a constant translational force due to the characteristics of human perception.

2. Related Force Displays for Mobility

Force displays can be categorized three types from the aspect of their fulcrum. One covers earth-grounded devices, such as PHANTOM[5], or SPIDAR[6]. Another is body-grounded, such as HapticGEAR[7]. The other covers non-grounded devices, such as angular momentum devices[8][9][10] or the jet-based device[11].

For wearable and mobile use, body-grounded devices or non-grounded devices have been adopted often. A major problem with body-grounded devices is passing the reactive force to the user. A major problem of the non-grounded devices is their inability to generate both constant and translational force; they can generate only short-time rotational force. Examples include GyroDisplay[9], which utilizes the gyro effect, and GyroCube[10], which presents a torque by using the change in angular momentum of a motor.

In this research, we implement the non-grounded style in a portable handheld device (Fig. 1). We highlight the fact that we utilize neither the gyro effect nor angular momentum; instead, we utilize the nonlinearity of human perception to generate force sensation, an approach has, up to now, been neglected.

3. Explanations of Perception Mechanism

This section explains our method how humans perceive a one-directional force although our force display generates bi-directional force.

The proposed force perception method subjects a mass to periodic translational motion; the mass is accelerated more rapidly in one direction than the other. If scaled



Fig. 1. Image of navigation by handling mobile phone

correctly, humans translate the asymmetric acceleration into a one-directional force because of their perception characteristics. While this force display system can be categorized as a non-grounded device (it has no fulcrum), it can generate constant force by repeating one cycle of motion.

In psychophysics, the relationship between stimulation and perception is known to match a psychometric function whose shape is an S-curve (sigmoid curve) as shown in Fig.2[12][13]. The integral of the psychophysical quantity into which the physical quantity (acceleration, in this case) is converted by the sigmoid curve does not necessarily equal zero even though the integral of the physical quantity is zero in one cycle of periodic motion. Given function $\alpha(t)$ of the acceleration change at time t , which meets condition:

$$\int_0^T \alpha(t) dt = 0 \quad (1)$$

where T is the cycle duration of the periodic motion, the total sense strength is calculated as:

$$\int_0^T \varphi \circ \alpha(t) dt \neq 0 \quad (2)$$

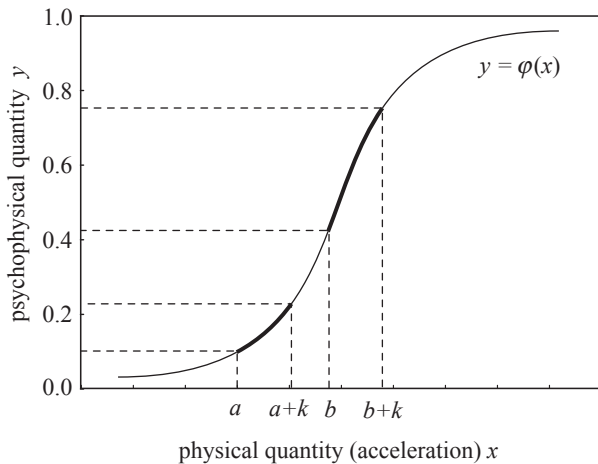


Fig. 2. Model of sigmoid curve of perception. Humans have nonlinear perception.

where $\varphi(x)$ is the nonlinear function of human perception that converts physical value x into a psychophysical value.

Furthermore, if we determine the area where the change of sense strength for acceleration value is large, it is not necessarily required to use high levels of acceleration. For example, the value of $\partial\varphi/\partial x|_{x=a+k} - \partial\varphi/\partial x|_{x=a}$ is larger than that of $\partial\varphi/\partial x|_{x=b+k} - \partial\varphi/\partial x|_{x=b}$ whereas the acceleration value b is larger than a and $\varphi(b)$ is larger than $\varphi(a)$. The important point is the *difference* in sense strength, not the *absolute values*; the proposed method does not require large levels of acceleration in order to realize the perception of a vector.

This phenomenon involves tactile and proprioceptive sensations as discussed below.

Reactive Characteristic of Muscle Spindle

The muscle spindle, which sends proprioceptive information about the muscle to the central nervous system, exhibits two reactions: static and dynamic. In the former, the sensory endings keep firing while the muscle tries to keep constant length. In the latter, the sensory endings fire when the muscle length changes and the level of excitation is strong when the change in length is comparatively small and sudden[14]. Therefore, short-time rapid acceleration changes invoke the dynamic reaction, which yields the virtual force.

Difference in Friction Force

The haptic display will slip over the skin in one direction if the peak acceleration in that direction exceeds the static friction force while the peak acceleration in the other direction does not. This may be a tactile clue that yields an equivalent force vector.

Temporal Masking

The much larger force in one direction, which is proportional to acceleration, "masks" the smaller force in the opposite direction, since they are located very closely in time. It follows that the user may not perceive the smaller force in the opposite direction, although the force component physically exists, thereby creating a sensation of a one-directional force. Prior temporal masking studies in haptics mainly focused on the cutaneous sensation (e.g., [15]), but masking is thought to also happen with regard to the force sensation.

4. Design of the Force Display

4.1. Generation Mechanism of Asymmetric Acceleration

The authors designed a mechanism to generate asymmetric acceleration as follows. To begin with, a circular motion at a constant speed is transformed into a

curvilinear motion by a swinging-block slider crank mechanism. By connecting the end point on the curvilinear motion and the point upon another slider which slides along a straight line, a reciprocating motion with asymmetric acceleration is generated. Figure 3 shows the prototype. In the prototype, the rotation of the motor makes the weights slide backwards and forwards with asymmetric acceleration. The device is composed of a single DOF (degree of freedom) mechanism. Since the prototype neither accelerates nor decelerates with the motor, its energy efficiency is high. Thus the mechanism is thought to be suitable for mobile and wearable computers which have limited energy reserves.

Figure 4 illustrates the mechanical configuration. The equation of motion of the weights is given by;

$$x = r \cos \theta + \mu(d - r \cos \theta) + \sqrt{l_2^2 - \{r(\mu - 1) \sin \theta\}^2} \quad (3)$$

where

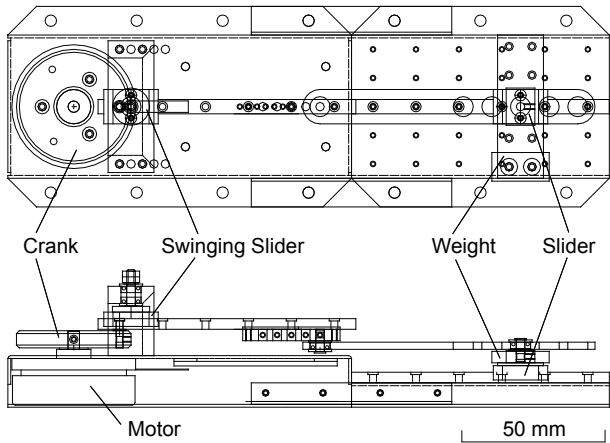
$$\mu = \frac{l_1}{\sqrt{r^2 + d^2 - 2rd \cos \theta}} \quad (4)$$

$x = OD$, $r = OB$, $d = OA$, $l_1 = BC$, $l_2 = CD$, and $\theta = AOB$.

Figure 4 shows the theoretical values of acceleration and velocity in the translational motion when the motor rotates at constant speed with cycle T [s]. The horizontal axis expresses time in units of rotation cycle T [s], and the vertical axis expresses acceleration and velocity.

The dynamics of the mechanism can be expressed as follows;

$$\begin{aligned} m_p \ddot{x} &= F_{Px} \\ &= m_E \ddot{x}_{Ex} - \left\{ m_A \ddot{x}_{Au} - \frac{\tau}{r} \sin(\theta - \phi) \right\} \cos \phi \\ &\quad + \frac{1}{\mu - 1} \left\{ \frac{\mu}{l_1} J_A \ddot{\phi} + \frac{\tau}{r} \cos(\theta - \phi) \right\} \sin \phi \end{aligned} \quad (5)$$



where

$$\phi = \pi - \arctan\left(\frac{r \sin \theta}{d - r \cos \theta}\right) \quad (6)$$

$$\begin{aligned} x_{Au} &= \left(1 - \frac{1}{\mu}\right)x_B + \frac{1}{\mu}x_C \\ &= \left(1 - \frac{1}{\mu}\right)r \{ \sin(\theta + \phi) - \cos(\theta - \phi) \} - d \cos \phi \end{aligned} \quad (7)$$

$$x_{Ex} = h_E \{ (1 - \mu)r \sin \theta + \mu d \} + (1 - h_E)x \quad (8)$$

τ represents the control torque at the crank. m_p , m_A , m_E represents the reciprocating mass, the mass of linkage BC, and that of linkage CD, respectively. The crank rotates at constant angular velocity; $\theta = \omega t$. J_A is the moment of inertia about point A. F_{Px} is the force on the slider. x_{Au} and x_{Ex} represent the positions of point A, and point E, respectively. $h_E = CD/DE$, $\phi = DAB$. The calculation is detailed in the Appendix.

4.2. Configuration of Prototype System

This system consists of the haptic display (virtual force display), a personal computer (CPU: Pentium4, 1.5 GHz), and a motor amplifier (DEC50/5; Maxon Motor). The motor in the virtual force display is a brushless DC motor (EC45 Flat motor; Maxon Motor), which has a power rating of 30 W, a weight of 88 g, and a maximum permissible rotation speed of 10,000 rpm. The power-supply voltage of the motor is DC18 V. The weight of the virtual force display except weights and the motor amplifier are approximately 230 g. The display is 70 mm wide \times 200 mm deep \times 48 mm high.

The personal computer is equipped with a D/A converter (PCI-3521; Interface Corporation) whose output range is 0-5 V unipolar and whose resolution is 12 bits. The personal computer controls the rotation speed of the motor in the virtual force display via its current.

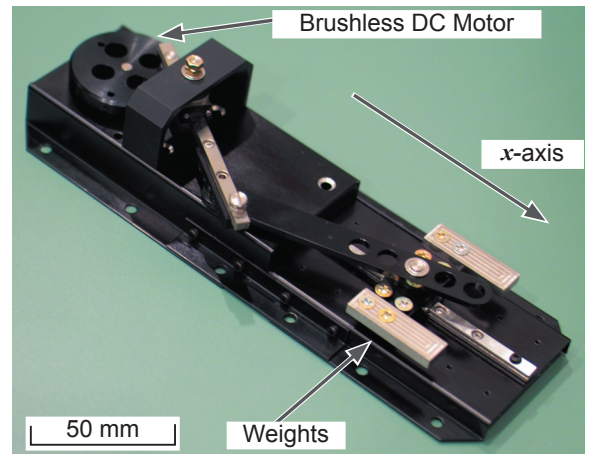


Fig. 3. Overview of a prototype of the haptic display

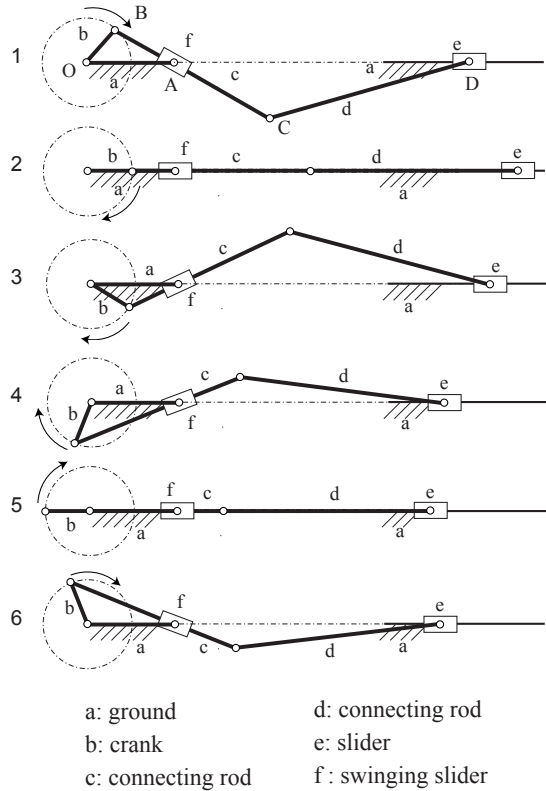
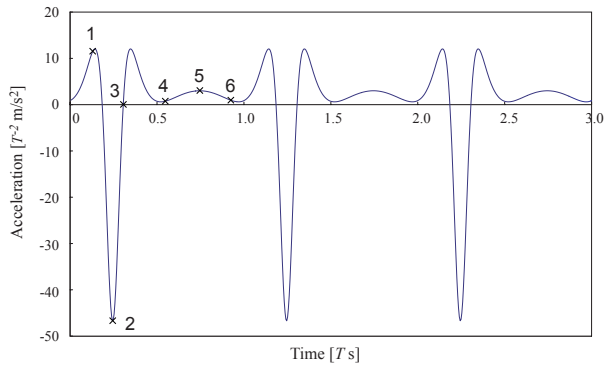
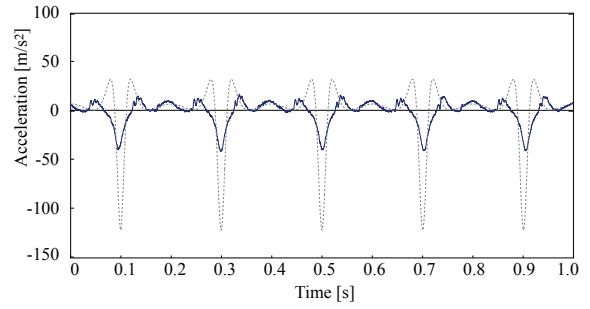


Fig. 4. Correspondence of the acceleration graph and the motion of slider *e*. Slider *e* slides backwards and forwards as crank *b* rotates. *f* oscillates around point *A*, and causes the slide to turn about the same point.

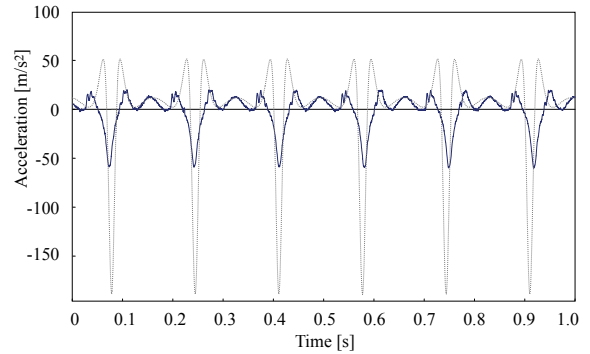
4.3. Evaluation of Prototype System

We measured the output acceleration of the virtual force display to confirm the basic mechanical properties. An acceleration sensor, whose weight including other electronic parts was 2 g, was adopted (ADXL210; Analog Devices Co.). The acceleration sensor was fixed to a weight in the virtual force display with double-sided tape, and the virtual force display was fixed to a base with double-sided tape. The mass of weights on the slider in the display was 20 g.

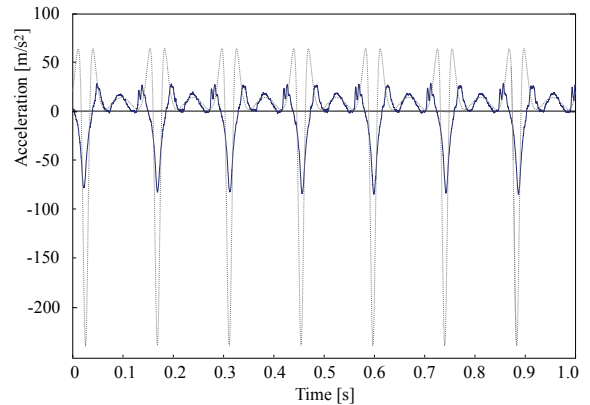
Figure 5 shows the measured acceleration values. Mechanical friction and sensor drift generated high-frequency noise, but peak moment and time ratio of



(a) 5 Hz



(b) 6 Hz



(c) 7 Hz

Fig. 5. Actual acceleration value of slider

acceleration change basically match the theoretical values.

5. Evaluation of Perceptual Characteristics

Our previous research revealed that humans could perceive the virtual force[16]. In this experiment, we determined the percent-correct scores at several motor rotational frequencies. Subjects made a single interval two-alternative forced-choice (2AFC) judgment on the force direction.

5.1. Methods

Three subjects, a man aged 28 (subject IT), a man aged 29 (subject GK), and a man aged 32 (subject TB), took

part voluntarily in this experiment. All subjects were right-handed. None of the subjects reported any known tactual impairments of their hands. Subject IT and GK had participated in pilot studies[16]. Subject TB was a naive participant. None were involved in the research project.

Figure 6 shows the experimental setup. Subjects were seated in front of the force display and adjusted the height of the chair to hold the device comfortably. The height of the device from the floor was about 1,000 mm. Two cubes made of acrylonitrile butadiene styrene (ABS) resin were attached to the virtual force display, and the subject held the closest case with the dominant hand (right hand, in this case). The method of grasping the device was constant throughout the experiment: the tips of the fingers wrapped around the side face of the case. To mask the visual and auditory cues, subjects wore eye masks and active noise-canceling headphones throughout the experiment. Responses were collected using three buttons in a ring mouse (Sigma, SGM-UK) that was held by the subjects with the nondominant hand. Correct-answer feedback was not provided during the experiment.

The direction of the translational motion was limited to one axis, forward and backward, by using a linear rail

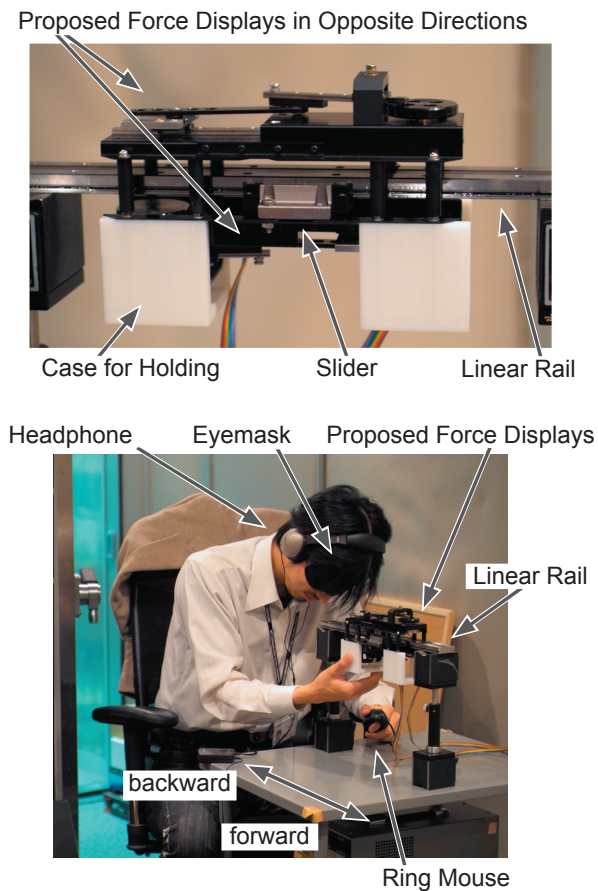


Fig. 6. View of experiment

(LWFF; the Nippon Thompson Co., Ltd). Two virtual force displays were fastened to a slider on the rail above and below; one was to present pulling force, the other was pushing force, they were switched by the digital output board (PCI-2702; Interface Corporation) in the computer shown in Figure 7. The length of the rail was 400 mm. The total mass of the weights on the slider in the virtual force display was 20 g.

We determined how often the perceived direction of movement matched the intended direction. The rotational frequency of the motor was altered (5, 10, 15, 20, or 40 Hz). Subjects indicated the direction of movement in 500 trials (100 trials at each frequency, fifty trials forward and fifty trials backward) with random order of direction and rotational frequency. The sequence of parameters was randomized for all subjects. The subjects were required to reply with one of the directions; the responses were either “feeling forward force (pushing relative to the ground)” to press the left button in the mouse or “feeling backward force (pulling relative to the ground)” to press the right button, answer such as “I’m not sure” were not accepted. Therefore, the chance performance level was 50 %. When the force vector was unambiguously perceivable, the correct answer rate was 100 %. In most psychology experiments, the threshold is set at 75 %. After pressing the button about direction, subject pressed the button on the index finger twice, one for confirmation, the other for final decision. If any button was pressed, verbal information synthesized by the computer (“forward”, “backward”, or “decision”) was played. The stimulation started two seconds after pressing the decision button, and was presented for two seconds just one time. In order to remove the influence of adaptation by long-term vibration and the influence of fatigue of muscle, the subject was given a two-minute break every 50 trials.

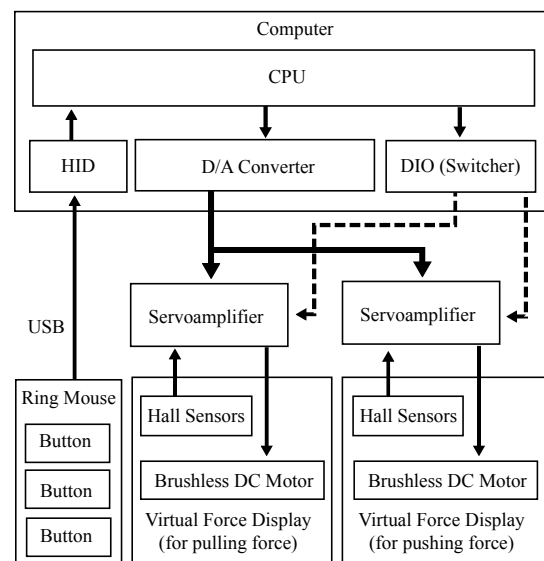
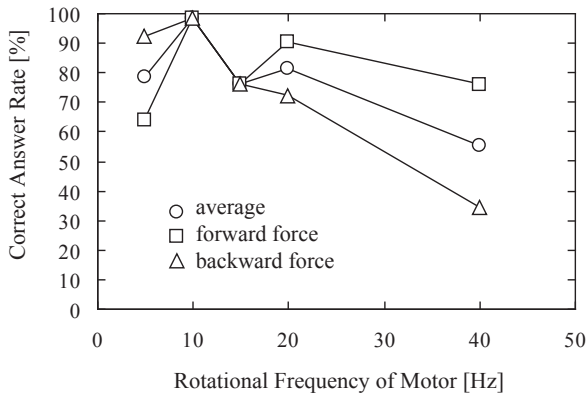


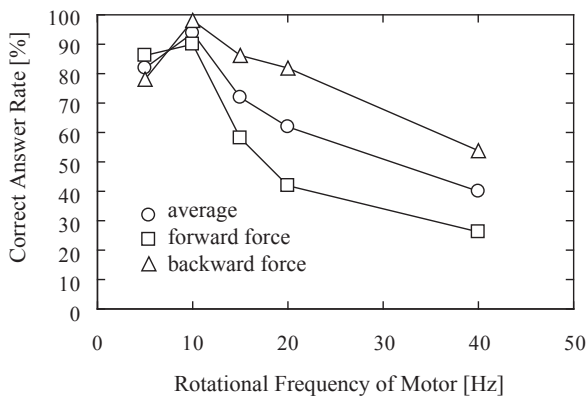
Fig. 7. System configuration of experiment

5.2. Results

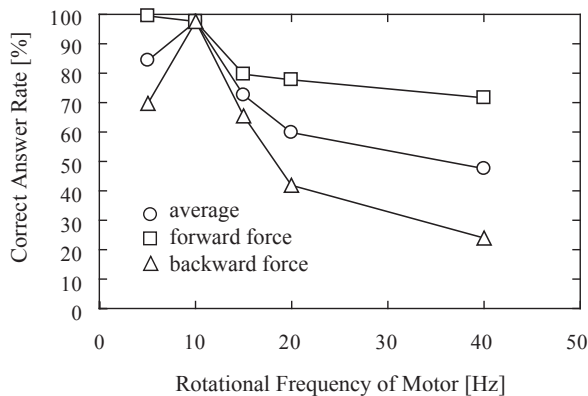
The experimental results of each subject are shown in Figure 8. The horizontal axis is the rotational frequency of motor in the force display, and the vertical axis is the percent-correct score. For all subjects, the frequency of 10 Hz yielded the best percent-correct scores (exceeding 90%), and 40 Hz worst (near the chance level).



(a) Subject IT



(b) Subject GK



(c) Subject TB

Fig. 8. Percentage-correct scores for subjects IT, GK, and TB (top, middle, and bottom row). Data from forward force, backward force, and total performance are shown by open squares, open triangles, and open circles, respectively.

We performed one-way analysis of variance (ANOVA) for the percent-correct scores at the five rotation frequencies of the motor. The result was statistically significant ($F(4,8)=28.20, p<.01$). Scheffe's test was used to compare each level. The results showed that 10 Hz was significant for 15 Hz ($p<.05$), 20 Hz and 40 Hz ($p<.01$). The performance of subject GK and TB decreased steadily with frequencies over 10 Hz. For subject IT, the tendency was almost the same except for a local minimum at 15 Hz. This tendency can be said to be independent of direction for all subjects.

For subject GK, percent-correct scores of backward force were better than those of forward force at over 10 Hz. For subjects IT and TB, on the other hand, percent-correct scores of forward force were better than those of backward force at over 10 Hz.

6. Discussion

6.1. Perception of Virtual Force Vector

Experimental results indicate that the frequency of acceleration change plays a more important role in establishing the perception of the vector than the amplitude of acceleration. This is because the percent-correct scores did not increase with the frequency of acceleration change (the rotational frequency of motor); the amplitude of acceleration is proportional to the square of the frequency of acceleration change. At frequencies higher than 10 Hz, the effect of the smaller force located closely in time cannot be neglected with regard to perception. The effect of the force amplitude will be investigated in a future experiment.

The vibration frequency range that maximizes the response of Meissner corpuscles (FA-I), which is in the shallow part of the skin and produces a vibratory sensation, is 5-40 Hz[17]. In addition, Tabot reported that Meissner corpuscles are most sensitive in the frequency range of approximately 30-40 Hz[18]. In our experiment, the Meissner corpuscles are thought to be the one of main receptors used in perceiving the virtual force vector on the skin since the frequencies used in the experiment ran from 5 to 40 Hz. Our results indicate that the strong response of Meissner corpuscles at 40 Hz made it difficult for the subjects to discriminate the difference of symmetric vibration and asymmetric acceleration change. This is consistent with the report from subjects that they felt the stimuli at 40 Hz as symmetric vibration.

Subjects also reported that they felt their arms moving. This suggests that reaction of muscle spindle and tendon might have contributed to the perception of the force vector. The reaction properties of muscle spindle and tendon for perception of the force vector will be investigated in future experiments.

6.2. Design of Multi-DOF Force Display

In this prototype, there was unnecessary force in unintended directions because of the movement of linkages. The unintended acceleration change was masked by the use of the linear rail in the experiments. Unwanted forces orthogonal to the desired direction can be countered by using a pair of two units with antiphase rotation.

One pair of units enables force display on one axis. Using two linearly independent pairs, or if one pair is combined with a rotational motor (e.g., stepper motor) for pan motion, makes it possible to create a virtual force in an arbitrary direction on a two dimensional plane.

6.3. Limitations

Our method does not suit for applications that requires precise force feedback such as touching virtual objects. Since the amplitude of the force perceived by the method depends on the users, we think our method fails to provide high fidelity rendering of the forces intended.

In this prototype, the amplitude of the virtual force is not large enough to move the body. Our method does not enforce any change in the behavior of humans. However, humans can feel the change of proprioception, which generates force feedback sensation, when the human actively moves his arm holding the force display in the same direction as the virtual force vector.

6.4. Scalability Issues

Our method was proposed for mobile and wearable force displays. Size is always an issue in mobile and wearable systems. In this section, we discuss the scalability of the system that uses our method.

It is easy to assume that a reduction in size would result in a reduction in the output force, especially amplitude of force which is proportional to both the weight of reciprocating mass and amplitude of acceleration. We will investigate the thresholds related to the trade-off between the amplitude of force and perception of the vector for miniaturization.

Note that we are not fixated on the slider crank; we plan to reduce the size of this force display by using other mechanisms that can realize the proposed asymmetric acceleration method.

7. Conclusion

This paper introduced a new simple force perception method that uses the tactual characteristics of humans to create a one-directional virtual force vector without a fulcrum. We designed and developed a handheld prototype that uses periodic prismatic motion to generate

asymmetric acceleration changes. We examined the impact of the rotational frequency of the driving motor on the perception of virtual force vectors. We found that the vector is well perceived at rotating frequencies around 10 Hz; results indicated that the frequency is more responsible for the perception of the vector than the amplitude. Future works include creating a multi-DOF force display, preventing the generation of force in unintended directions, solving the problem of the acceleration change due to gravity, and improving wearability and mobility by miniaturization.

Acknowledgements

Thanks are due to Dr. Kawabuchi for his assistance in the hardware development phase.

References

- [1] C. D. Chapman, M. D. Heath, D. A. Westwood, and E. A. Roy, "Memory for Kinesthetically Defined Target Location: Evidence for Manual Asymmetries", *Brain and Cognition*, Vol. 46, Nos. 1-2, pp. 62-66, 2001.
- [2] S. Ertan, C. Lee, A. Willets, H. Tan, and A. Pentland, "A Wearable Haptic Navigation System", *Proceedings of the 2nd International Symposium on Wearable Computers*, Pittsburgh, PA, pp. 164-165, October 1998.
- [3] D. Ross and B. Blasch, "Wearable Interfaces for Orientation and Wayfinding", *ACM Conference on Assistive Technologies*, Arlington, VA, pp. 193-200, November 2000.
- [4] T. Amemiya, J. Yamashita, K. Hirota, and M. Hirose, "Virtual Leading Blocks for the Deaf-Blind: A Real-Time Way-Finder by Verbal-Nonverbal Hybrid Interface and High-Density RFID Tag Space", *Proceedings of IEEE Virtual Reality Conference 2004*, Chicago, IL, pp. 165-172, March 2004.
- [5] T. H. Massie and J. K. Salisbury, "The PHANToM Haptic Interface: A Device for Probing Virtual Objects", *Proceedings of the ASME Winter Annual Meeting, Symposium on Haptic Interfaces for Virtual Environment and Teleoperator Systems*, Vol. 55-1, pp.295-300, Chicago, IL, November 1994.
- [6] M. Sato, "SPIDAR and Virtual Reality", *World Automation Congress, IFMIP-043*, pp. 1-7, 2002.
- [7] M. Hirose, K. Hirota, T. Ogi, H. Yano, N. Kakehi, M. Saito, and M. Nakashige, "HapticGEAR: The Development of a Wearable Force Display System for Immersive Projection Displays", *Proceedings of Virtual Reality 2001 Conference*, Yokohama, Japan, pp. 123-130, March 2001.
- [8] H. Ando, M. Sugimoto, and T. Maeda, "Wearable Moment Display Device for Nonverbal Communication", *IEICE Transactions on Information and Systems*, Vol. E87-D, No. 6, pp. 1354-1360, 2004.
- [9] H. Yano, M. Yoshie, and H. Iwata, "Development of a Non-Grounded Haptic Interface Using the Gyro Effect", *Proceedings of HAPTICS 2003*, Los Angeles, CA, pp. 32-39, March 2003.
- [10] Y. Tanaka, S. Masataka, K. Yuka, Y. Fukui, J. Yamashita, and N. Nakamura, "Mobile Torque Display and Haptic Characteristics of Human Palm", *Proceedings of ICAT 2001*, Tokyo, Japan, pp. 115-120, December 2001.

- [11] H. Gurocak, S. Jayaram, B. Parrish, and U. Jayaram, "Weight Sensation in Virtual Environments Using a Haptic Device With Air Jets", *Journal of Computing and Information Science in Engineering*, Vol. 3, No. 2, pp. 130-135, June 2003.
- [12] P. H. Lindsay and D. A. Norman, "Human Information Processing: An Introduction to Psychology", Academic Press, 1977.
- [13] S. S. Stevens, "Psychophysics: Introduction to Its Perceptual, Neural, and Social Prospects". John Wiley and Sons, 1975.
- [14] N. Kakuda and M. Nagaoka, "Dynamic response of human muscle spindle afferents to stretch during voluntary contraction", *Journal of Physiology*, Vol. 513, pp. 621-628, 1998.
- [15] H. Z. Tan, C. M. Reed, L. A. Delhorne, N. I. Durlach, and N. Wan, "Temporal Masking of Multidimensional Tactile Stimuli", *Journal of the Acoustical Society of America*, Vol. 114, No. 6, pp. 3295-3308, December 2003.
- [16] T. Amemiya, H. Ando, and T. Maeda, "Virtual Force Display: Direction Guidance using Asymmetric Acceleration via Periodic Translational Motion", *Proceedings of IEEE World Haptics Conference 2005*, pp. 619-622, Pisa, Italy, March 2005.
- [17] R. S. Johansson, U. Landstrom, and R. Lundstrom, "Responses of Mechanoreceptive Afferent Units in the Glabrous Skin of the Human Hand to Sinusoidal Skin Displacements", *Brain Research*, Vol. 244, pp. 17-25, 1982.
- [18] W. H. Talbot, I. D. Smith, H. H. Kornhuber, and V. B. Mountcastle, "The Sense of Flutter-Vibration: Comparison of the Human Capacity With Response Patterns of Mechanoreceptive Afferents From the Monkey Hand", *Journal of Neurophysiology*, Vol. 31, pp. 301-334, 1967.

Appendix

We derive the equation in Section 4.1 as follows;

The moment of inertia J_O about point O can be neglected because the second order derivative of $\theta = 0$.

$$J_O \ddot{\theta} = \tau + rF_B$$

$$\therefore \tau = -rF_B \quad (9)$$

where F_B is tangential force as shown in Figure 9. The equation of motion at the u -axis of linkage BC can be expressed as;

$$m_A \ddot{x}_{Au} = F_B \sin(\theta - \phi) + F_{Cu} \quad (10)$$

and the equation of moment around point A of linkage BC can be expressed as;

$$J_A \ddot{\phi} = F_B \frac{l_1}{\mu} \cos(\theta - \phi) - F_{Cv} (1 - \frac{1}{\mu}) l_1 \quad (11)$$

where J_A is the moment of inertia about point A. The equation of motion at the x -axis of linkage CD can be

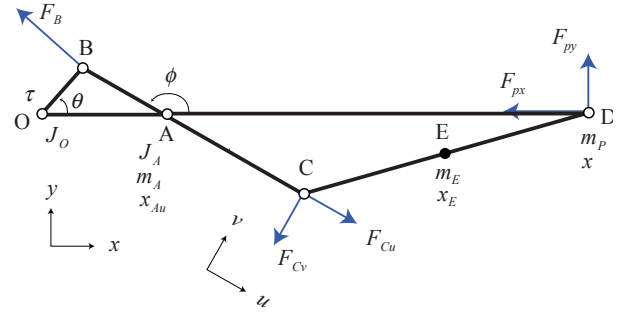


Fig. 9. Force and moment diagram for linkage

expressed as;

$$m_E \ddot{x}_{Ex} = -F_{px} - F_{Cu} \cos \phi - F_{Cv} \sin \phi \quad (12)$$

Using equation (9), (10), (11), and (12), the equation (5) can be derived in a straight forward manner.